A Bivalent Tarantula Toxin Activates the Capsaicin Receptor, TRPV1, by Targeting the Outer Pore Domain

Christopher J. Bohlen,[1,3] Avi Priel,[1,3] Sharleen Zhou,[2] David King,[2] Jan Siemens,[1,4,*] and David Julius[1,*]

[1]Department of Physiology, University of California, San Francisco, 600 16th Street, San Francisco, CA 94143-2140, USA
[2]Howard Hughes Medical Institute Mass Spectrometry Laboratory, University of California, Berkeley, Berkeley, CA 94720-3202, USA
[3]These authors contributed equally to this work
[4]Present address: Max-Delbrück-Centrum für Molekulare Medizin, Berlin-Buch, Robert-Rössle-Strasse 10, 13125 Berlin, Germany
*Correspondence: jan.siemens@mdc-berlin.de (J.S.), julius@cmp.ucsf.edu (D.J.)
DOI 10.1016/j.cell.2010.03.052

SUMMARY

Toxins have evolved to target regions of membrane ion channels that underlie ligand binding, gating, or ion permeation, and have thus served as invaluable tools for probing channel structure and function. Here, we describe a peptide toxin from the Earth Tiger tarantula that selectively and irreversibly activates the capsaicin- and heat-sensitive channel, TRPV1. This high-avidity interaction derives from a unique tandem repeat structure of the toxin that endows it with an antibody-like bivalency. The "double-knot" toxin traps TRPV1 in the open state by interacting with residues in the presumptive pore-forming region of the channel, highlighting the importance of conformational changes in the outer pore region of TRP channels during activation.

INTRODUCTION

Venoms from spiders, snakes, fish, cone snails, and scorpions contain an evolutionarily honed pharmacopeia of natural toxins that target membrane receptors and ion channels to produce shock, paralysis, pain, or death. Toxins evolve to interact with functionally important protein domains, including agonist binding sites, ion permeation pores, and voltage-sensing domains, making them invaluable reagents with which to probe mechanisms underlying receptor and channel activation or modulation (Hille, 2001). In addition to well-known and deadly small-molecule toxins, such as tetrodotoxin from puffer fish or saxitoxin from dinoflagellates, there exists a tremendous diversity of genetically encoded peptide toxins that have likewise proven invaluable for elucidating the structure, function, and physiological properties of membrane ion channels (Catterall et al., 2007; Escoubas and Rash, 2004; Miller, 1995; Swartz, 2007; Terlau and Olivera, 2004). Prototypical of this class is α-bungarotoxin, a 74 amino acid-long peptide from elapid snakes that binds to the agonist pocket of nicotinic acetylcholine receptors with pico-molar potency and an essentially irreversible rate of dissociation.

As such, α-bungarotoxin has been an essential tool in the purification, localization, and functional analysis of both native and recombinant acetylcholine-gated channels (Tsetlin et al., 2009).

While genetically encoded peptide toxins exhibit substantial sequence and functional diversity, many share common structural elements—most notably the presence of several intramolecular disulfide bonds that limit conformational flexibility to enhance both specificity and avidity of toxin-target interactions. Included among such peptides are a large group of so-called inhibitor cysteine knot (ICK) toxins that are typically 25–50 residues in length and share a conserved gene structure, precursor organization, and three-dimensional fold. ICK peptides are commonly found in venoms from cone snails, spiders, and scorpions, where they are estimated to account for 10^5–10^6 unique toxin sequences (Craik et al., 2001; Zhu et al., 2003). Repeated use of the ICK motif through evolution presumably reflects the "fitness" of this structural motif for generating large collections of stable and functionally diverse molecules that have the capacity to interact with a wide array of membrane protein partners. In essence, the venom sacs of these organisms can be viewed as functionally focused combinatorial peptide libraries. Not surprisingly, the vast majority of peptide toxins remain uncharacterized insofar as structure, physiologic effects, or molecular sites of action (Escoubas and Rash, 2004; Terlau and Olivera, 2004).

Among ICK toxins, charybdotoxin and hanatoxin (from scorpion and tarantula venom, respectively) are the best characterized. Both inhibit voltage-gated (K_v) potassium channels, but elegant mutagenesis and biophysical studies have shown that they do so in mechanistically distinct ways (Miller, 1995; Swartz, 2007). Charybdotoxin binds to the so-called pore-loop domain of the channel located between the fifth and sixth transmembrane domains (S5 and S6), thereby blocking ion permeation directly (Goldstein et al., 1994; Gross et al., 1994; MacKinnon et al., 1990; Yu et al., 2005). In contrast, hanatoxin interacts primarily with residues in the C-terminal half of the third transmembrane region (S3b), which together with S4 and the intervening extracellular loop forms a flexible helix-turn-helix domain whose movements contribute to voltage-dependent gating (Alabi et al., 2007; Swartz and MacKinnon, 1997). Upon binding, hanatoxin inhibits movement of this voltage sensor region during

membrane depolarization, thereby favoring the closed state (Lee et al., 2003; Phillips et al., 2005). The analysis of charybdotoxin- and hanatoxin-K_v channel interactions has been key to formulating and testing models of ion permeation and voltage sensor movement, respectively, as well as in delineating interactions of these functionally important protein domains with drugs and membrane lipids (Milescu et al., 2009; Schmidt and MacKinnon, 2008; Swartz, 2008).

The mammalian TRP channel family consists of >30 members, many of which are known to form tetrameric cation channels in vivo or when heterologously expressed (Ramsey et al., 2006; Venkatachalam and Montell, 2007). Physiological roles for many TRP channels remain enigmatic; however, several are known to contribute to sensory signaling, including thermosensation, nociception, and pain. Chief among these is TRPV1, which is activated by capsaicin (the main pungent ingredient in "hot" chili peppers), extracellular protons, and other inflammation agents, as well as noxious heat (>43°C) (Julius and Basbaum, 2001). Despite their rather distinct physiological roles, TRP and voltage-gated ion channels likely resemble one another in so far as overall transmembrane topology and tetrameric subunit organization, consistent with the fact that TRP channels exhibit some (albeit modest) degree of voltage sensitivity (Brauchi et al., 2004; Matta and Ahern, 2007; Voets et al., 2004). With this in mind, we recently asked whether spider or scorpion venoms also contain toxins that target TRP channels, particularly those expressed on primary afferent sensory nerve fibers of the pain pathway. As a result, we discovered a group of three ICK peptides (dubbed vanillotoxins, VaTx1, 2, and 3) from the "Trinidad Chevron" tarantula (*Psalmopoeus cambridgei*) that activate TRPV1 to produce robust inflammatory pain (Siemens et al., 2006). Interestingly, vanillotoxins exhibit appreciable sequence similarity to hanatoxin, and some vanillotoxins (VaTx1 and VaTx2) also inhibit $K_v2.1$, furthering speculation that TRP and voltage-gated channels resemble one another in regard to structure and/or gating mechanisms.

Vanillotoxins are excellent pharmacological probes, but their relatively fast dissociation rates limits their usefulness as biochemical tools for studying TRP channel structure. Here, we describe a toxin from the Earth Tiger tarantula that serves as a specific and irreversible TRPV1 agonist. The toxin contains two independently folded ICK domains, endowing it with an antibody-like bivalency that results in extremely high avidity for its multimeric channel target, making it a powerful biochemical tool for probing TRP channel function. We found that this toxin binds to and traps TRPV1 in the open state via association with the pore-forming region of the channel, rather than the voltage sensor equivalent region near the S3 and S4 helices. These and other observations support a critical role for the pore-forming domain in TRP channel gating and suggest that conformational changes in the outer pore may be more important than previously appreciated.

RESULTS

Multiple Spider Species Target TRPV1 Channels

The Chinese bird spider, *Ornithoctonus huwena* (a.k.a. Earth Tiger), is a particularly large and aggressive Old World tarantula
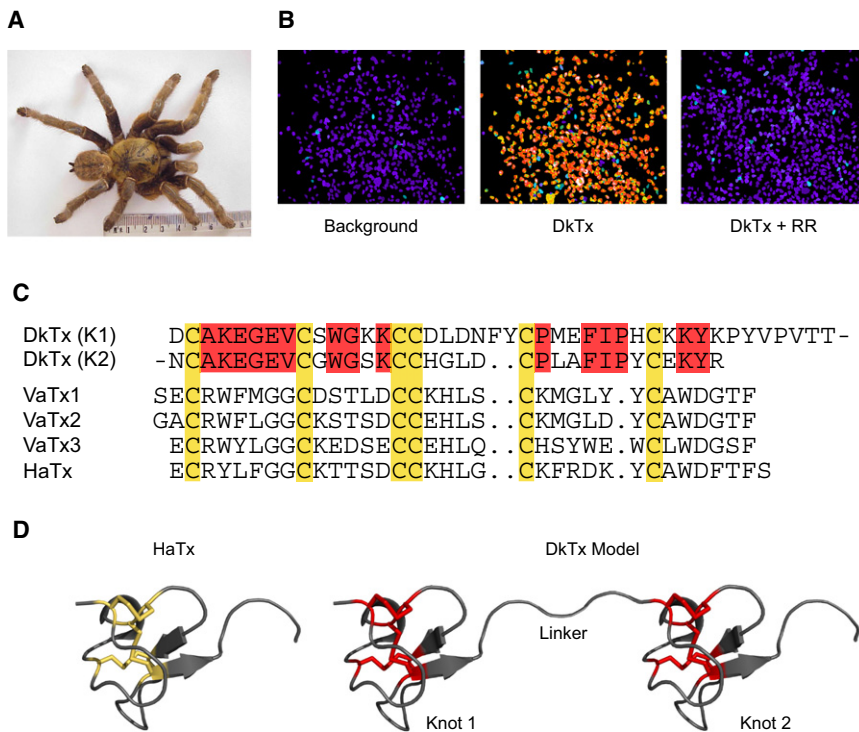
that inhabits deep underground burrows within tropical regions of southern China and Vietnam (Figure 1A) (Liang, 2004). Bites are generally not lethal to humans, but they can produce substantial pain and inflammation. Like the Trinidad Chevron, crude venom from this spider activates recombinant TRPV1, suggesting that it contains one or more peptide toxins that target nociceptors as part of its chemical defense strategy (Siemens et al., 2006). We purified the major active component to homogeneity using calcium imaging as a functional readout (Figure 1B and Figure S1A available online).

Many peptide toxins, including VaTx1 and VaTx2, are known to target multiple channels subtypes. To assess specificity of the purified *O. huwena* toxin, we examined the effect of a relatively high dosage (2 μM) on a panel of TRP (TRPV2, TRPV3, TRPV4, TRPA1, and TRPM8), ligand-gated (5-HT₃R-A and P2X₂), and voltage-gated ($K_v1.2$, $K_v2.1$, and $K_v4.3$, $Ca_V1.2$, $Ca_V3.3$, and $Na_V1.7$) channels (Figure S1B), many of which are expressed in sensory neurons. No discernable effect was observed when DkTx was applied to oocytes or HEK293 cells expressing any of these channels. In keeping with this apparent selectivity for TRPV1, calcium-imaging experiments with cultured trigeminal neurons showed toxin-evoked calcium influx in a subset of neurons corresponding to the capsaicin-sensitive cohort. Moreover, this response was absent in cultures derived from TRPV1-deficient mice (Figure 2A).

O. huwena Toxin Is a Bivalent ICK Peptide

The absorbance and migration profile of *O. huwena* toxin on reversed-phase matrix suggested that the active component is hydrophobic and peptidic in nature. Given its rather large size (monoisotopic mass of 8521.9 Da) and relative paucity in venom, we could only obtain a partial sequence of the toxin by de novo peptide sequencing. To circumvent this problem, we prepared total RNA from venom glands of *O. huwena* spiders and used this material to clone complementary DNAs (cDNAs) encoding the mature toxin. Indeed, the predicted sequence thusly obtained matched the observed mass of the full-length toxin and proteolytically derived fragments. Moreover, the native toxin contained a C-terminal amidated arginine, consistent with the fact that cDNA sequence predicts transfer of an amide group from a glycine residue in the n + 1 position of the precursor peptide.

Although the *O. huwena* toxin contains a pattern of cysteine residues that conforms to the ICK motif seen in the vanillotoxins, the toxin bears little sequence similarity with the vanillotoxins, suggesting that *P. cambridgei* and *O. huwena* spiders have independently developed TRPV1 agonists through a process of convergent evolution. Most strikingly, the *O. huwena* toxin is approximately twice the size of the vanillotoxins and consists of two head-to-tail ICK unit repeats separated by a short linker (Figure 1C). ICK units adopt a characteristically compact and rigid structure, and thus we propose that the *O. huwena* toxin forms two independently folded domains connected by a kinked tether (Figure 1D). As this *O. huwena* peptide presents an example of a toxin containing tandemly repeated ICK motifs, we have dubbed it the "double-knot" toxin (DkTx).

A

B

Background   DkTx   DkTx + RR

C

```
DkTx (K1)   DCAKEGEVCSWGKKCCDLDNFYCPMEFIPHCKKYKPYVPVTT-
DkTx (K2)   -NCAKEGEVCGWGSKCCHGLD..CPLAFIPYCEKYR
VaTx1       SECRWFMGGCDSTLDCCKHLS..CKMGLY.YCAWDGTF
VaTx2       GACRWFLGGCKSTSDCCEHLS..CKMGLD.YCAWDGTF
VaTx3       ECRWYLGGCKEDSECCEHLQ..CHSYWE.WCLWDGSF
HaTx        ECRYLFGGCKTTSDCCKHLG..CKFRDK.YCAWDFTFS
```

D

HaTx   DkTx Model

Knot 1   Linker   Knot 2

Figure 1. The Chinese Bird Spider Produces a Bivalent TRPV1 Toxin

(A) The Chinese bird spider (*Ornithoctonus huwena*) is a large terrestrial tarantula with a leg span of up to 12 cm. It is found primarily in the Guangxi province of China (photo courtesy of Chuck Kristensen, Spider Pharm).

(B) Purified DkTx toxin evokes robust calcium increases in HEK293 cells expressing the rat TRPV1 channel. Coapplication of ruthenium red (RR; 10 μM), a nonselective TRP channel pore blocker, inhibits toxin-evoked responses. Purple denotes low resting cytoplasmic calcium, and orange indicates calcium increase.

(C) DkTx is a member of the ICK peptide family. Other than the highly conserved arrangement of cysteine residues (highlighted in yellow), DkTx shows no obvious sequence similarity with other ICK peptides, including the vanillotoxins (VaTx1–3) and hanatoxin (HaTx).

(D) DkTx consists of two ICK lobes (Knot 1 and Knot 2) separated by a short linker region. The nuclear magnetic resonance solution structure of HaTx (Takahashi et al., 2000) served as a template for a hypothetical model of DkTx, showing the conserved disulfides in yellow for HaTx and red for DkTx (generated with PyMOL, http://www.pymol.org/). These tandemly repeated lobes show significant sequence identity (see C), suggesting that they arose by gene duplication. See also Figure S1.

DkTx Is a Virtually Irreversible TRPV1 Activator

The apparent structure of DkTx suggests that it behaves as a bivalent ligand, in which case it should demonstrate an exceptionally high avidity for its multimeric target, reminiscent of an antibody-antigen complex. To test this prediction, we carried out whole-cell patch-clamp recordings from capsaicin-sensitive trigeminal neurons to assess the persistence of DkTx-evoked currents. Application of purified DkTx (1 μM) produced characteristic outwardly rectifying, ruthenium red-blockable currents resembling those elicited by capsaicin (Figure 2B). However, we observed a striking difference between these two agonists in regard to the kinetics of the response. Whereas capsaicin-evoked currents returned to baseline within 10 s of washout, those elicited by DkTx persisted for minutes with minimal decline in magnitude (Figure 2B).

To characterize this phenomenon in greater detail, we compared off rates of various agonists by recording from TRPV1-expressing HEK293 cells. As expected, responses to capsaicin and extracellular protons (pH 5.5) declined rapidly with washout, exhibiting τ_{off} = 0.17 and 0.005 min, respectively. In contrast, currents evoked by purified vanillotoxins showed substantially slower decay rates, with τ_{off} ranging from 1.6 to 2.5 min (Figure 2C), as expected for relatively large and molecularly complex peptide agonists. Remarkably, currents elicited by DkTx were even more persistent, verging on irreversible, thereby precluding meaningful measurements of τ_{off} (Figure 2C). This phenomenon was independent of concentration since currents persisted for >15 min when elicited by 0.2 μM or 2 μM toxin (Figure 2C). In either case, > 50% of maximal toxin-evoked

response remained after an extended washout period. In light of these observations, we conclude that DkTx exhibits a high avidity for TRPV1, presumably reflecting association of this bivalent ligand with the homotetrameric channel so as to form an extremely stable complex exhibiting very slow rates of toxin dissociation.

Bivalence Accounts for Irreversible Toxin Action

To test the prediction that the tandem-repeat nature of DkTx accounts for its high avidity for TRPV1, we generated a modified toxin that could be proteolytically separated to yield the component ICK lobes for direct functional comparison. To achieve this, we introduced a Genenase I cleavage site (-HYR-) into the linker region of the mature DkTx sequence (Figure 3A) and expressed both wild-type (DkTx) and modified (DkTx-HYR) peptides recombinantly by using a bacterial expression system. Heterologous expression of ICK toxins is notoriously difficult to achieve, owing to the low probability of proper disulfide bond formation (Bulaj and Olivera, 2008). Nonetheless, a substantial amount (40 mg/l culture) of total unfolded toxin peptide was produced, of which a workable fraction (1%) could be refolded to yield chromatographically well-behaved peptide (Figure S2A). Native DkTx, recombinant DkTx, and recombinant DkTx-HYR all activated TRPV1 with similar potency (EC$_{50}$ = 0.23, 0.14, and 0.24 μM, respectively; Figures 3B and 3D), eliciting essentially irreversible, outwardly rectifying, ruthenium red-blockable currents (Figure 3C).

Incubation of purified DkTx-HYR with Genenase I resulted in quantitative cleavage into the N- and C-terminal ICK peptides
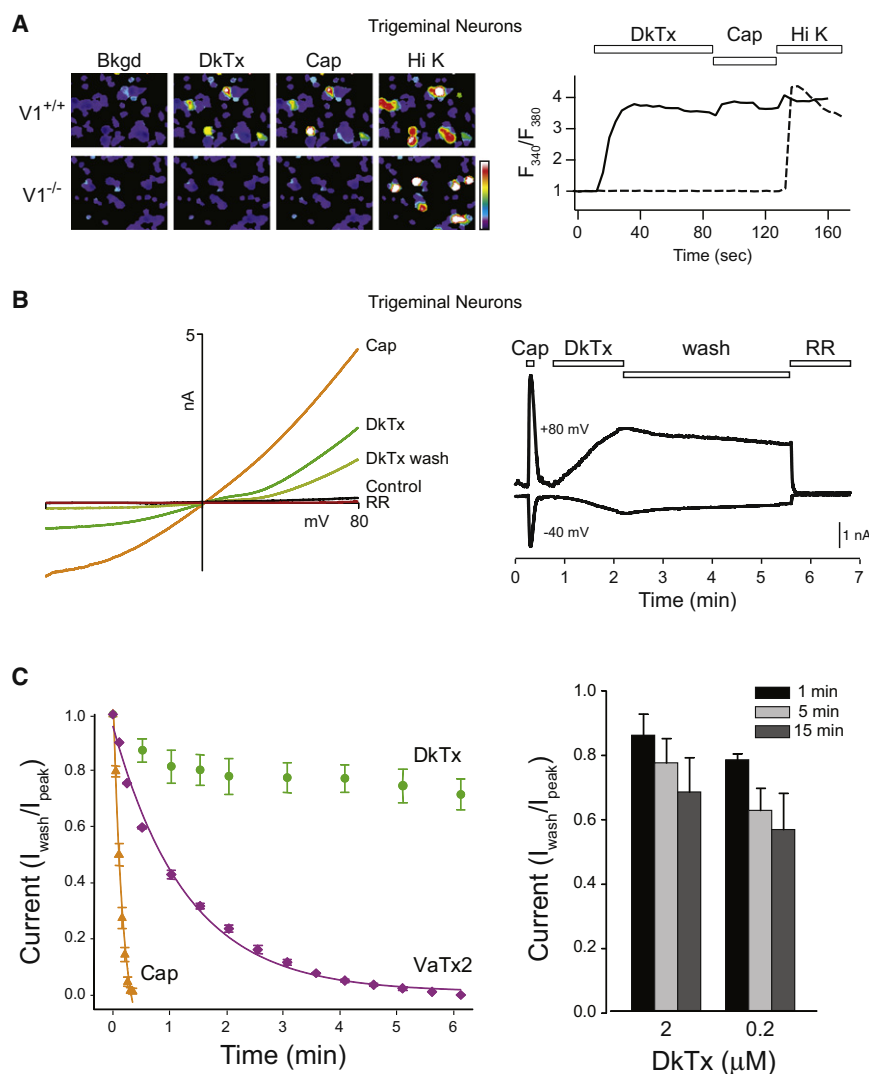
Figure 2. DkTx Is a Selective and Irreversible TRPV1 Activator

(A) Trigeminal sensory neurons from wild-type ($V1^{+/+}$) or TRPV1-deficient ($V1^{-/-}$) mice were examined for responses to capsaicin (1 μM; Cap) and DkTx (5 μM) via ratiometric calcium imaging. Depolarization with high extracellular potassium (75 mM; Hi K) identified all neurons in the field. Left: pseudocolor images of Fura-2-loaded cells (color bar indicates relative change in fluorescence ratio, with purple and white denoting lowest and highest cytoplasmic calcium). Right: average ratiometric calcium responses as a function of time. Solid and dashed lines represent responses from wild-type and TRPV1-deficient trigeminal neurons, respectively. Note lack of DkTx-evoked response by TRPV1-deficient neurons (n ≥ 50 cells per trace).

(B) Both capsaicin (Cap; 1 μM) and DkTx (2 μM) elicited outwardly rectifying, ruthenium red (RR; 4 μM) blockable currents in cultured mouse trigeminal neurons (recorded in whole-cell patch-clamp configuration). Current-voltage relationships and representative current trace are shown at left and right, respectively. Note persistence of DkTx-evoked response even after 3–4 min washout period.

(C) Left: relative washout rates were determined for electrophysiological responses to saturating doses of capsaicin (1 μM; orange), VaTx2 (2 μM; purple), or DkTx (2 μM; green). Individual points represent fractional current remaining as measured by whole-cell patch-clamp recording from TRPV1-expressing HEK293 cells (V_h = +80 mV). When washout was complete, a time constant of decay could be determined by exponential fit of the data (τ_{off} = 0.17 min and 1.3 min for capsaicin and VaTx2, respectively) (n = 4–7 cells per point). Right: plot of fractional DkTx-evoked current remaining after a 1, 5, or 15 min washout period as determined for two different toxin concentrations (n = 5–9 cells per bar). Average values represent mean ± standard error of the mean (SEM).

(K1 and K2, respectively), which were subsequently separated and purified by reversed-phase chromatography, as confirmed by mass spectrometry (Figure S2B). With these reagents in hand, we could assess relative potencies and kinetics of TRPV1 activation. Clearly, separation of DkTx-HYR into K1 and K2 single-knot peptides was associated with a substantial drop in potency when compared to the intact toxin, as evidenced by a 5- and 50-fold increase in EC_{50} values for K2 and K1, respectively (Figure 3D). This was accompanied by a marked increase in cooperativity (indicated by a shift in hill coefficient from ∼1 to 4), suggesting that more single-knot toxins must bind per TRPV1 complex to promote channel activation. Moreover, we also observed a striking difference in the time course of toxin action, such that responses to K1 or K2 declined rapidly upon washout and showed no sign of the persistent currents elicited by the parental DkTx-HYR (Figure 3E). Coadministration of K1 and K2 produced the same response observed with K2 alone (the more potent of the two peptides) (data not shown), indicating

that these ICK lobes must be physically tethered to achieve the potency and irreversibility of native or recombinant double-knot toxin.

Are sequence differences in the similar but nonidentical K1 and K2 essential for irreversible TRPV1 activation? To address this issue, we generated a modified toxin in which the K2 sequence was replaced by K1, thereby producing a toxin with two identical ICK lobes. The K1-K1 double knot had higher potency than K1 alone (EC_{50} = 0.44 μM) and resembled wild-type DkTx in its ability to elicit irreversible channel activation (Figure S3). This ability to generate a high-avidity toxin by simply duplicating one knot suggests that each lobe of K1-K1 (and by analogy, K1 and K2 of native DkTx) interacts with equivalent sites on separate channel subunits to produce a stable, high-avidity complex.

DkTx Binds to and Locks TRPV1 in the Open State

Given the bivalent nature of DkTx, we asked whether the toxin must bind simultaneously to multiple channels to effect
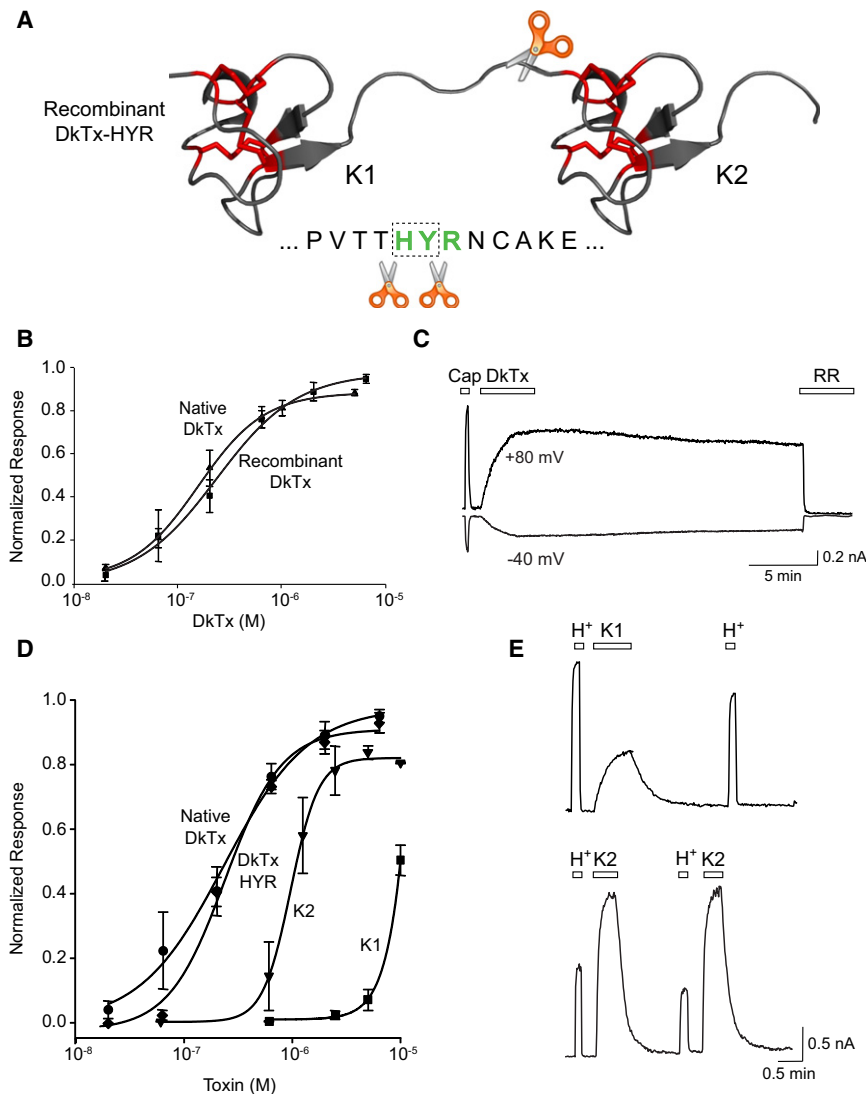
Figure 3. Bivalency Is Required for Persistent Toxin Action

(A) Schematic depicts location of engineered protease (Genenase I) cleavage site in recombinant DkTx.

(B) Native and recombinant DkTx are equipotent as determined by calcium imaging with TRPV1-expressing HEK293 cells. Values are normalized to maximal capsaicin- (10 μM) evoked responses (n = 3–4 wells per point).

(C) Whole-cell patch-clamp recording from TRPV1-expressing HEK293 cells shows that recombinant DkTx (2 μM) produces persistent, ruthenium red- (RR) blockable membrane currents comparable in magnitude to those elicited by capsaicin (1 μM).

(D) Dose-response analysis (carried out as in B) shows that native and recombinant DkTx containing the Genenase I cleavage site (HYR) are equipotent. Knot 1 and Knot 2 peptides (K1 and K2), derived from Genenase I cleavage of HYR, are active but significantly less potent (EC_{50} = 8.9 and 0.97 μM, respectively). Values are normalized to maximal capsaicin- (10 μM) evoked responses (n = 3–4 wells per point).

(E) Representative whole-cell patch-clamp recordings (+80 mV) from TRPV1-expressing HEK293 cells showing responses to extracellular protons (H^+; pH 5.5), K1 (20 μM; top trace), or K2 (20 μM; bottom trace) peptides. Note the rapidly reversible (i.e., non-persistent) nature of K1- or K2-evoked responses following washout.

Average values represent mean ± SEM. See also Figures S2, S3, S4, and S5.

persistent activation. To address this question, we analyzed single-channel responses in excised outside-out membrane patches taken from TRPV1-expressing HEK293 cells (Figure S4). Like other vanillotoxins (Siemens et al., 2006), DkTx activated the channel in the outside-out but not inside-out configuration, consistent an extracellular site of action (Figure S5A). Using a saturating dose of capsaicin (1 μM), we first identified patches containing a single functional TRPV1 channel (Figure S4A). Subsequent exposure to recombinant DkTx produced single-channel events whose unitary conductance was within 15% of that evoked by capsaicin (103 and 118 pS, respectively), but whose mean open times were dramatically longer (Figures S4A and S5B). These results demonstrate that irreversible gating can be achieved through interaction of DkTx with a single TRPV1 channel.

Consistent with whole-cell recordings, single-channel records showed that persistent activation by DkTx is time dependent (Figure S4A). Interestingly, onset of the persistent phase could be substantially accelerated when toxin was applied in the presence of capsaicin. Thus, even brief coapplication of capsaicin and DkTx converted flickering capsaicin-evoked responses to nonflickering openings that persisted long after washout of both agonists (Figure S4B). Consistent with this, we observed similar behavior at the macroscopic (whole-cell) level, where coapplication of toxin and capsaicin enhanced both the rate and efficiency with which irreversible currents developed (Figure S5C). Taken together, these findings suggest that DkTx binds to TRPV1 in an open state-dependent manner, trapping it there to produce irreversible currents.

Toxin Activation Is Specified by Residues within the Pore-Forming Region of TRPV1

Based on the known mechanism of hanatoxin action and presumed similarities between TRP and voltage-gated channels, we initially assumed that vanillotoxins would mediate their effects through interaction with the topologically equivalent domain (S3b-S4) of TRPV1. However, alanine scanning of this region (residues 517 through 550) failed to identify residues that contribute significantly to VaTx3- or DkTx-evoked channel activation (see below). We therefore adopted a different strategy for identifying the site(s) of TRPV1-toxin interaction.
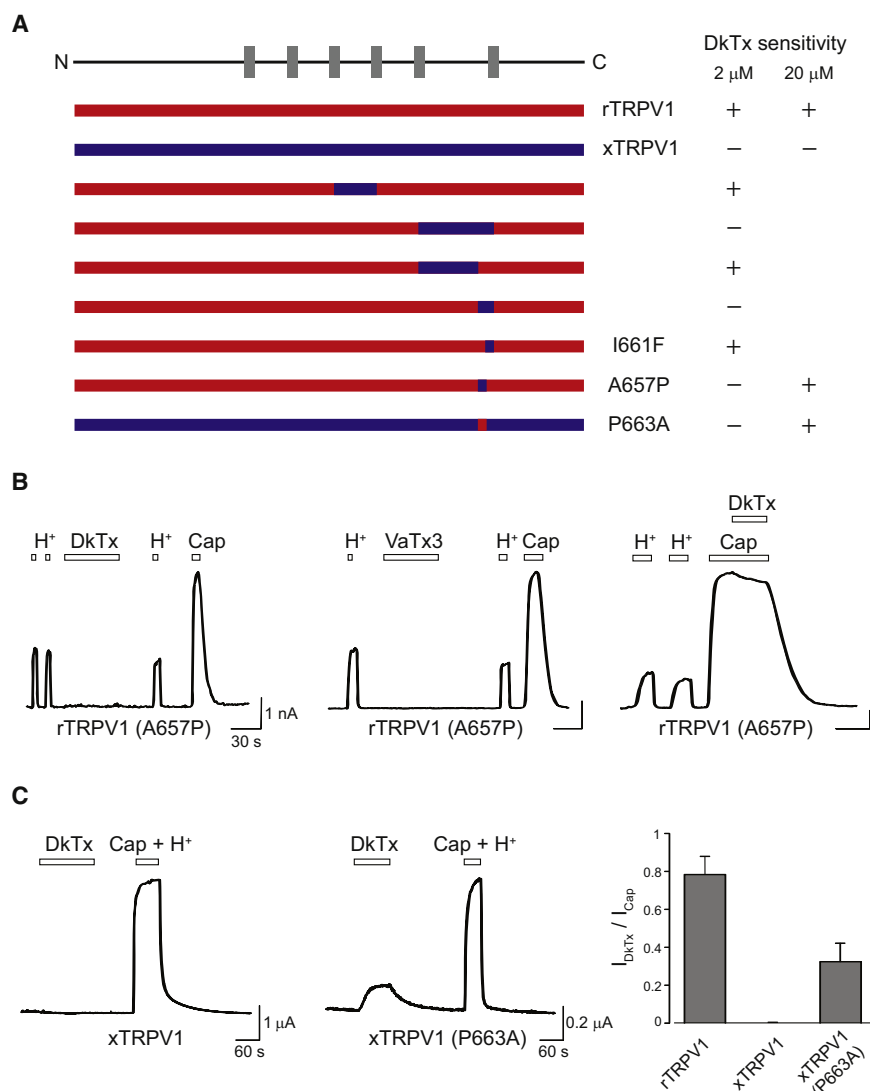
Figure 4. The TRPV1 Pore Domain Specifies Toxin Sensitivity

(A) Chimeric channels were generated between rat and *Xenopus* TRPV1 orthologs (red and blue bars, respectively) on the basis of the location of putative transmembrane domains (gray bars). All chimeras shown were activated by capsaicin. Selective sensitivity of rat TRPV1 to DkTx mapped to residue A657, which, when replaced by the equivalent residue from the frog channel (P663), led to dramatically reduced toxin sensitivity.

(B) Representative whole-cell patch-clamp recording (+80 mV) from HEK293 cells expressing the rat TRPV1 (A657P) mutant showed selective loss of DkTx (2 μM; left) or VaTx3 (2 μM; center) sensitivity. In contrast, sensitivity to capsaicin (Cap; 1 μM) and extracellular protons (H+; pH 5.5) was retained. Coapplication of capsaicin and DkTx (right) failed to produce persistent channel activation.

(C) Representative two-electrode voltage-clamp recordings (+80 mV) from *Xenopus* oocytes expressing wild-type frog TRPV1 channel (left) shows specific insensitivity to DkTx (20 μM) versus capsaicin and protons (50 μM at pH 5.5). The frog TRPV1 P663A mutant (center) showed acquisition of toxin sensitivity. Note the reversibility of toxin-evoked current. The graph at the right shows average toxin responses for wild-type rat, wild-type frog, and mutant frog (P663A) channels normalized to capsaicin-evoked responses (n = 3–5 cells per bar; average values represent mean ± SEM).
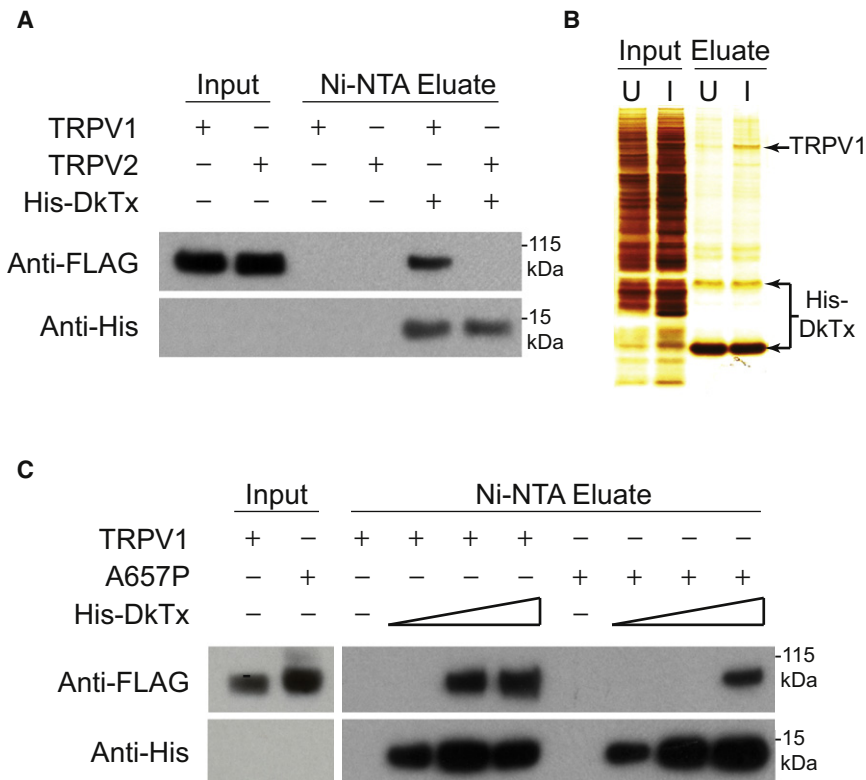
See also Figure S6.

Detailed dose-response analysis revealed a 100-fold drop in DkTx potency at rTRPV1 (A657P) mutant compared to the wild-type channel. Although toxin-evoked responses were observed at high DkTx concentrations, currents returned to baseline shortly after toxin washout (Figure S6A). Thus, changes at this position diminish both toxin potency and persistence, suggesting that A657 is located within or near a site of toxin-channel interaction. For all other 18 amino acid substitutions, only A657W showed a substantial loss of toxin sensitivity compared to capsaicin (Figure S6B). Mutants bearing charged or polar side chains did not respond to either agonist, suggesting that uncharged or hydrophobic side chains at this position are required for normal channel function and that the toxin does not tolerate the bulkiest residues, proline, and tryptophan.

To determine whether the A657 residue is both necessary and sufficient to account for the species-specific toxin sensitivity, we asked whether the reciprocal mutant (P663A) conferred toxin responsiveness to frog TRPV1. The xTRPV1 (P663A) mutant is poorly expressed compared to the wild-type channel but nevertheless showed robust responses to DkTx at concentrations (20 μM) that had no effect on the wild-type frog channel (Figure 4C). Thus, all other amino acid differences between the

Sensory receptors show substantial functional diversification as organisms evolve to inhabit different ecological niches. This most often manifests as differential sensitivity to physiological stimuli, which can be exploited to delineate receptor domains that contribute to ligand binding or activation. Indeed, this strategy has been especially fruitful for pinpointing residues that are required for activation or inhibition of TRP channels by chemical ligands (Chou et al., 2004; Chuang et al., 2004; Gavva et al., 2004; Jordt and Julius, 2002; Phillips et al., 2004). We therefore asked whether ICK toxins activate TRPV1 orthologs from nonmammalian species. We found that *X. laevis* frog TRPV1 (xTRPV1) is insensitive to VaTx3 or DkTx, although it responds to other stimuli, such as capsaicin or extracellular protons. By analyzing a series of rat-frog TRPV1 chimeras and point mutants, we traced this differential response profile to a single amino acid located at the extracellular boundary of the S6 domain (Figure 4A). Thus, rat TRPV1 harboring the frog residue at this site (A657P) retained sensitivity to capsaicin and low pH but was unresponsive to VaTx3 or DkTx (Figure 4B).

A

B

C

Figure 5. DkTx Binds Directly to TRPV1 via Association with the Pore Domain

(A) DkTx affinity resin retains detergent solubilized TRPV1, but not TRPV2, protein. Recombinant His-tagged DkTx was immobilized on nickel-affinity (Ni-NTA) resin, to which affinity-purified FLAG-tagged TRPV1 or TRPV2 protein (Input) was subsequently applied. After extensive washing, toxin-channel complexes were eluted and analyzed by western blotting using anti-FLAG or anti-His antisera to detect channel or toxin protein, respectively. Complexes were observed with TRPV1, but not TRPV2 input, and were not detected with Ni-NTA beads lacking toxin.

(B) Crude membrane extracts (Input) from uninduced (U) or induced (I) TRPV1-HEK293 cells were applied to DkTx-coupled resin. Bound material (Eluate) was recovered and analyzed by silver staining, showing substantial enrichment of TRPV1-toxin complexes over other membrane proteins.

(C) TRPV1 A657P mutant binds less avidly to DkTx affinity resin. Purified wild-type (TRPV1) and mutant (A657P) protein were analyzed for toxin binding as described in (A) using resins with increasing DkTx substitution (wedges depict 3-fold concentration range). Mutant (A657P) channel protein was retained only at the highest toxin density.

rat and frog channels (Figure S6C) must have only minor effects on toxin sensitivity. Taken together, these results suggest that toxin-TRPV1 association is specified by residues within the pore-forming domain of the channel, near the S6 region.

**The TRPV1 A657P Mutation Disrupts DkTx Binding**

Our electrophysiological results are consistent with a model in which peptide toxins promote TRPV1 gating through a direct interaction with the pore-forming region of the channel complex. To assess binding directly, we immobilized histidine-tagged recombinant DkTx on nickel resin and asked whether this toxin affinity column could retain purified TRPV1 protein. Detergent solubilized and purified FLAG-tagged TRPV1 was incubated with DkTx-coupled resin, which was then washed extensively (30 min) before elution of the retained proteins. Indeed, DkTx-coupled (but not control untreated) resin depleted TRPV1 quantitatively from the detergent extract and elution released the channel in complex with DkTx (Figure 5A). Toxin-channel association could also be observed via the converse protocol, in which TRPV1 was immobilized on a FLAG immunoaffinity column to which soluble DkTx was applied (data not shown). Importantly, no interaction was observed with either protocol when TRPV2 was used in place of TRPV1, attesting to the specificity of toxin binding (Figure 5A).

To further demonstrate the specificity of toxin-channel binding, we performed a similar experiment by using crude detergent solubilized membrane extracts from TRPV1-expressing HEK293 cells, rather than purified channel protein. Although TRPV1 represents only a small fraction of total membrane

protein (even after induced overexpression), it was greatly enriched in the material eluted from the toxin-coupled resin (Figure 5B). In fact, the purity of this sample rivaled that generally obtained by FLAG purification, supporting a direct and specific biochemical interaction between DkTx and TRPV1. Consistent with its decreased toxin sensitivity, we found that the TRPV1 (A657P) mutant protein was retained on the DkTx affinity column, but only when toxin density exceeded that required for efficient purification of the wild-type channel (Figure 5C). These biochemical results support our conclusions from physiological experiments that toxin interacts directly with residues in the pore-forming region of TRPV1.

Multiple Sites within the TRPV1 Outer Pore Domain Are Critical for Toxin Activation

To further delineate a footprint of toxin-channel interaction, we asked whether mutations in other residues within the S5-S6 domain would abrogate toxin-evoked TRPV1 activation. Indeed, alanine scanning of this region (residues 592–665) revealed three sites (I599, F649, and F659) where alanine substitutions produced marked diminution of toxin responses while retaining capsaicin sensitivity (Figures 6A and 6B and Figure S7). Together with A657, these residues delineate a potential toxin interaction site bracketed by the extracellular boundaries of S5 and S6, corresponding to the outer pore domain (Figure 6D). At high toxin concentrations ($\geq 20~\mu M$), residual responses can be observed with each of these single point mutations (Figure S6C and data not shown), whereas a quadruple mutant (I599A, F649A, A657P, F659A) completely eliminates toxin sensitivity
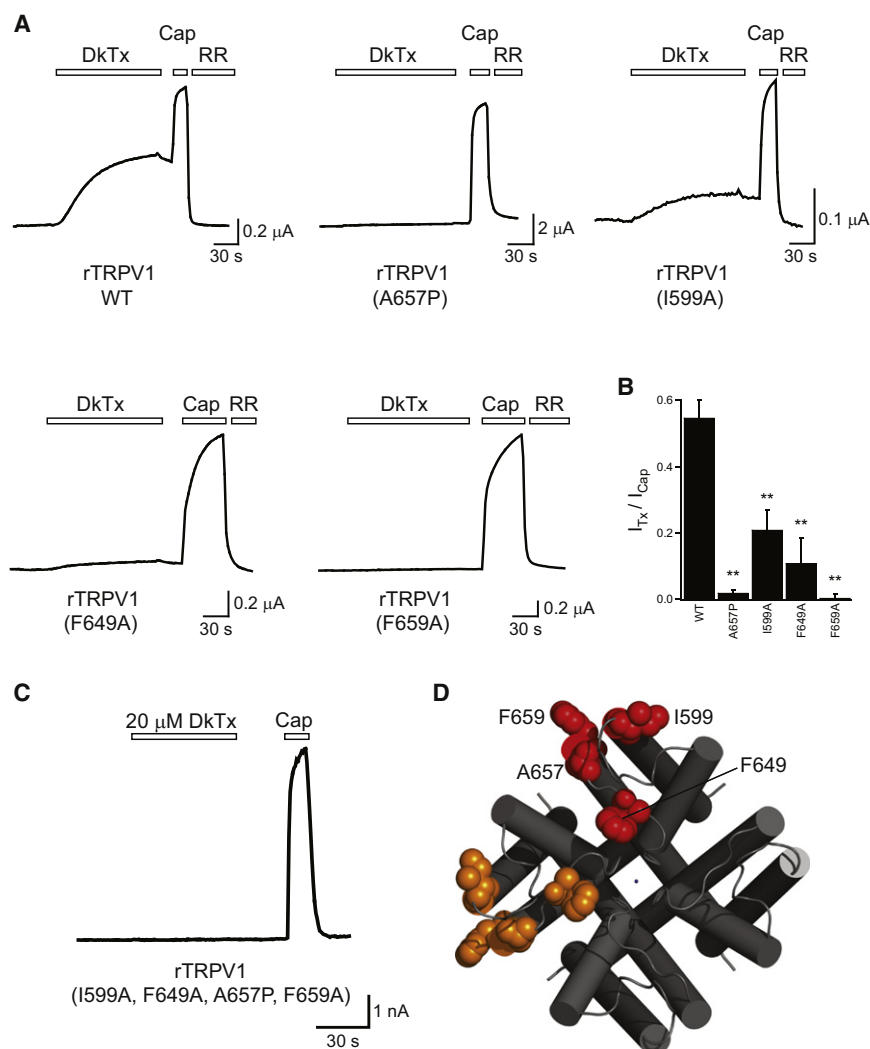
Figure 6. Mutagenesis Outlines a DkTx Footprint on the Extracellular Face of TRPV1

(A) Representative voltage-clamp recordings (V_h = +80 mV) from oocytes expressing wild-type or mutant rat TRPV1 channels in response to double-knot toxin (DkTx; 1.5 μM), then capsaicin (Cap; 3 μM), followed by block with ruthenium red (RR; 80 μM).

(B) Quantitative comparison of toxin-evoked responses normalized to a maximal capsaicin-evoked response. Note the substantial and significant (n = 5–8 cells per mutant; average values represent mean ± SEM; p < 0.01, one-way ANOVA) decrement in toxin sensitivity for all mutants shown versus wild-type TRPV1.

(C) Whole-cell patch-clamp recording from a transfected HEK293 cell expressing a TRPV1 channel containing all four outer pore mutations shows complete loss of toxin sensitivity even when challenged with DkTx at a concentration (20 μM) exceeding the EC_{50} by 100-fold.

(D) Putative locations of residues required for DkTx sensitivity are mapped onto a model pore domain on the basis of the structure of the bacterial potassium channel, KcsA (Doyle et al., 1998). Amino acid side chains of TRPV1 residues I599, F649, A657, and F659 are shown in color, depicting a potential footprint of toxin binding. Red and orange groups correspond to bivalent DkTx attachment sites on adjacent channel subunits. Such an interaction may also be mediated through interaction with non-adjacent (orthogonal) subunits.

See also Figure S7.

(Figure 6C). This result suggests that these sites impact toxin binding in nonidentical ways and that the outer pore domain plays a dominant and necessary role in mediating toxin sensitivity.

ICK Toxins Interact Differentially with TRPV1 and K$_v$2.1

In contrast to our findings with TRPV1-activating toxins, hanatoxin has been shown to inhibit K$_v$ channels by associating with the S3b-S4 voltage-sensing paddle domain, thereby retarding its movement during depolarization. We therefore asked whether VaTx1, which both activates TRPV1 and inhibits K$_v$2.1, also interacts with the S3b-S4 region of the latter. To answer this question, we examined three K$_v$2.1 voltage sensor domain mutants (I273Y, F274R, and E277K) that have been previously shown to disrupt hanatoxin-mediated inhibition of this channel (Li-Smerin and Swartz, 2000). Two of these mutations (F274R, and E277K) eliminated VaTx1-mediated inhibition (even at toxin concentrations exceeding the IC_{50} value for wild-type K$_v$2.1), whereas the third (I273Y) had a modest effect (Figure 7B). These results strongly suggest that VaTx1, like hanatoxin, targets the

voltage sensor of K$_v$2.1 to mediate channel inhibition. VaTx1 activation of TRPV1, on the other hand, was abolished by the TRPV1 (A657P) mutation in the pore domain (Figure 7A). Thus, vanillotoxins likely interact with different regions of TRP and K$_v$ channels in their capacity to serve as agonists or antagonists, respectively.

DISCUSSION

Genetically Encoded Bivalency as a Feature in Toxins

To date, over 1000 ICK peptides have been characterized, demonstrating substantial variation in length, amino acid sequence, number and configuration of disulfide bonds, and posttranslational modification (Gelly et al., 2004; Terlau and Olivera, 2004). However, unlike other members of this extended peptide family, DkTx contains tandemly repeated ICK units. Our results show that each unit can exist as structurally and functionally independent entities which, when combined, synergize to produce a ligand of exceedingly high avidity. The irreversible action of DkTx should translate into excruciating and prolonged pain, perhaps in keeping with the reputation of the *O. huwena* spider as an aggressive and fearsome creature (Liang, 2004). Indeed, persistent activation of TRPV1 will be accompanied by intense pain and robust neurogenic inflammation that will cease
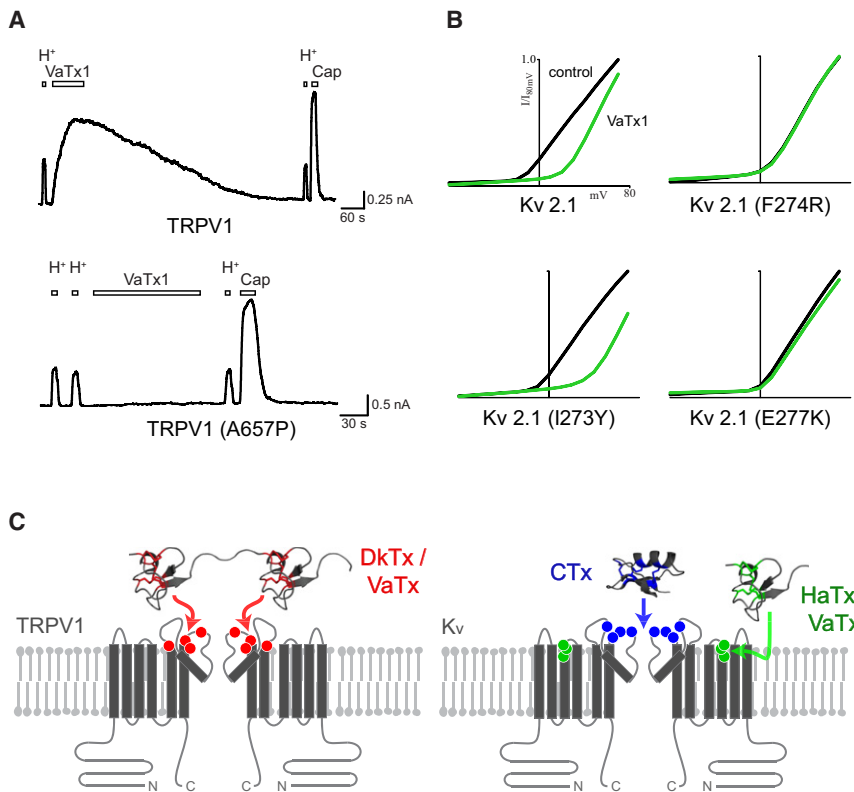
Figure 7. VaTx1 Targets Distinct Regions of K$_v$2.1

(A) Representative whole-cell patch-clamp recording (+80 mV) from HEK293 cells expressing rat TRPV1 (top) or the TRPV1 (A657P) mutant (bottom) show VaTx1 (100 μM) activation of the wild-type, but not the mutant, channel. Capsaicin (Cap; 1 μM) and extracellular protons (H$^+$; pH 5.5) are shown for reference.

(B) Two-electrode voltage-clamp recordings from *Xenopus* oocytes expressing rat K$_v$2.1 voltage-gated potassium channels in the absence (black) and presence (green) of the vanillotoxin VaTx1 (20 μM). Two mutations (F274R and E277K) that are known to abrogate the inhibitory effect of hanatoxin on this channel also eliminated VaTx1-evoked inhibition, whereas a third (I273Y) had no substantial effect on VaTx1 action (n = 3–5 cells per trace).

(C) Model of the transmembrane topology of TRPV1 (gray bars represent transmembrane helices) highlighting residues (red dots) that are crucial for double-knot toxin (DkTx) activation. In the simplest scenario, the two knots of DkTx bind to two equivalent sites on multiple subunits of the same channel. Kv channels likely possess the same overall transmembrane topology as TRPV1 but interact with ICK toxins in different ways. For example, charybdotoxin (CTx) binds within the ion permeation path to block ion flux, and voltage-modulator toxins, such as hanatoxin (HaTx), target the voltage sensor to modify gating properties (blue and green dots represent mutations that attenuate CTx and HaTx inhibition, respectively). Our findings suggest that single-knot vanillotoxins (VaTx) also target the S3–S4 helices of K$_v$ channels, but they activate TRPV1 through the pore region.

only upon desensitization and/or neurotoxic injury to the primary afferent fiber.

Venoms contain hundreds of toxins that evolve through a process of gene duplication and divergence (Diao et al., 2003; Duda and Palumbi, 1999). In some cases, individual toxin peptides can posttranslationally associate through noncovalent or covalent (e.g., disulfide linkage) interactions to form higher-order complexes that target multimeric receptors (Roy et al., 2010; Walker et al., 2009). In the case of DkTx, gene duplication has apparently produced a dimer-like structure within a single coding region. With the advent of new high-throughput methods for sequencing complex mixtures of ICK peptides (Ueberheide et al., 2009), it will be interesting to see whether this double-knot motif represents a general evolutionary strategy for producing tandemly repeated toxins that target homomeric and heteromeric receptors with high avidity. In any case, much as polymer-linked small molecules have been used to probe channel structure (Kramer and Karpen, 1998), DkTx inspires a biosynthetic strategy for the rational design of multivalent peptide ligands (agonists or antagonists) using the ICK fold as a template. Indeed, our engineered K1-K1 peptide demonstrates the feasibility of this approach. Thus, just as hanatoxin and charybdotoxin have served as essential tools for defining the basic functional components of voltage-gated channels, DkTx and genetically engineered derivatives provide analogous new biochemical tools for dissecting the unique properties of TRP channels and facilitating structural studies.

ICK Toxins Target Distinct Domains of TRP and Voltage-Gated Ion Channels

Peptide toxins, particularly those within the ICK family, modulate voltage-gated channels through two main mechanisms. One, exemplified by hanatoxin or β-scorpion toxin, involves association of the toxin with the S3b-S4 domain of K$_v$ or Na$_v$ channels, respectively, trapping the voltage sensor so as to favor the closed or open state (Catterall et al., 2007; Cestèle et al., 1998; Li-Smerin and Swartz, 1998; Sokolov et al., 2008; Swartz, 2007). The second, exemplified by charybdotoxin, involves a more passive mechanism in which the toxin binds to the S5-S6 region of closed or open K$_v$ channels to occlude passage of ions through the pore (Goldstein et al., 1994; Gross et al., 1994; MacKinnon et al., 1990; Yu et al., 2005). Vanillotoxins, including DkTx, suggest another mechanism, in which gating equilibrium is modulated by interaction with the pore domain (rather than the S3b-S4 region) to promote channel opening (rather than occlusion) (Figure 7C). This is reminiscent of hydrophobic small-molecule modulators such as dihydropyridines or batrachotoxin, which alter voltage-gated calcium or sodium channel activity through interactions with intramembrane sites close to or within the S6 helix (Catterall et al., 2007; Wang and Wang, 2003). While vanillotoxin activation of TRPV1 likewise involves interaction with residues in the S5-S6 region, these are predicted to reside on the extracellular face of the plasma membrane, rather than deep within the lipid bilayer.

The vanillotoxin, VaTx1, serves as both a $K_v2.1$ inhibitor and a TRPV1 activator. VaTx1 resembles hanatoxin in so far as predicted fold and primary sequence, and thus it makes sense that mutations within the S3b-S4 region of $K_v2.1$ abrogate both hanatoxin- and VaTx1-mediated inhibition, consistent with a common mechanism of toxin action. In contrast, we were surprised to find that vanillotoxins (VaTx1 and DkTx) interact with a completely different domain of TRPV1, namely the outer pore region, which has little, if any, influence on hanatoxin-K_v interaction (Alabi et al., 2007; Li-Smerin and Swartz, 2000). Our evidence disfavoring a role for the S3-S4 domain in TRPV1-vanillotoxin interaction rests on "negative" results, namely an inability to identify mutations within this region that disrupt toxin-evoked channel activation, despite extensive scanning. Thus, it remains formally possible that the S3-S4 region of TRPV1 plays some role in vanillotoxin binding. However, our ready identification of functionally important sites within S5-S6, together with the chimeric channel experiments, strongly suggests that the outer pore domain constitutes a major and essential locus underlying toxin sensitivity. Thus, vanillotoxins recognize distinct, nonoverlapping sites on different channels to produce activation or inhibition. Presumably, this differential interaction of ICK toxins with TRP and voltage-gated channels highlights the relative importance of these domains to channel gating. Moreover, the ability of some toxins (such as VaTx1) to modulate both types of ion channels may conspire to enhance neuronal depolarization.

The TRPV1 Outer Pore Domain as a Key Locus of Channel Activation

Our electrophysiological and biochemical studies indicate that residues at the extracellular face of the TRPV1 S6 domain engage in DkTx binding (Figure 7C). Because DkTx binds preferentially to TRPV1 in the open state, it follows that the pore domain of the channel probably undergoes substantial conformational rearrangement during gating, consistent with recent mutagenesis studies indicating that the outer pore region is critical for gating of TRPV channels (Grandl et al., 2008; Myers et al., 2008; Yeh et al., 2005). This stands in contrast to K_v channels, where the outer pore domain has been suggested to remain relatively stationary during the gating process (Long et al., 2005; Tombola et al., 2006). Thus, while TRP and voltage-gated channels likely share gross architectural features, they must also possess unique structural elements that enable them to fulfill different physiological roles, such as detection of membrane voltage versus thermal or chemical stimuli. Future structural studies will be necessary to understand the full extent of similarities and differences in the gating process for these distinct ion channel families.

EXPERIMENTAL PROCEDURES

Native DkTx Purification and Cloning

DkTx peptide was purified from crude *O. huwena*, venom (Spider Pharm) by reversed-phase chromatography, similarly to as described (Siemens et al., 2006). The gene sequence of mature DkTx was obtained from RNA extracted from *O. huwena* venom glands. A degenerate primer derived from DkTx N-terminal peptide sequence was used to perform 3′ RACE (SMART-RACE kit, Clontech). A conserved "prepro" sequence found in some *O. huwena* toxin cDNAs (Diao et al., 2003) and the reverse-complement of the determined 3′ untranslated region (UTR) sequence were used as PCR primers to amplify the full coding sequence for the mature toxin.

Recombinant Toxin Expression and Purification

Each toxin construct was expressed in *E. coli* with a cleavable hexahistidine tag at the N terminus. Protein was extracted from inclusion bodies with 8 M urea and refolded by dialysis against refolding buffer (2.5 mM reduced glutathione, 0.25 mM oxidized glutathione, 20 mM Tris [pH 8.5]), and properly folded peptide was purified by reversed-phase chromatography. His-tagged toxin was tested for activity and used for binding assays, but for all other experiments, the hexahistidine tag was removed with TEV protease, and toxin was purified by reversed-phase chromatography. For cleavage into K1 and K2, purified DkTx-HYR was digested with Genenase I (New England Biolabs), and digestion products were separated by reversed-phase chromatography. All protein concentrations were determined by predicted extinction coefficient at 280 nm.

Molecular Biology

Full-length TRPV1 (rat), FLAG-TRPV1 (rat), FLAG-TRPV2 (rat), and FLAG-TRPV1 (A657P) were stably expressed in Flp-in T-REX 293 cells (Invitrogen). For transient expression, channels were cloned into pMO or pFROG3 and transfected into HEK293t cells with Lipofectamine 2000 (Invitrogen). *X. laevis* TRPV1 coding region was cloned from RNA isolated from trigeminal and dorsal root ganglia for use in 3′ and 5′ RACE (SMART-RACE kit, Clontech).

Cell Culture, Calcium Imaging, and Electrophysiology

Calcium imaging was performed as described (Siemens et al., 2006). For electrophysiology of acutely dissociated trigeminal neurons, the extracellular solution contained 150 mM NaCl, 2.8 mM KCl, 1 mM $MgSO_4$, 1 mM $CaCl_2$, 10 mM HEPES, and 0.01 mM tetrodotoxin (pH 7.4). The pipette solution contained 130 mM K-gluconate, 15 mM KCl, 4 mM NaCl, 0.5 mM $CaCl_2$, 1 mM EGTA, 10 mM HEPES, and 3 mM MgATP (pH 7.2). For whole-cell recordings from HEK293 cells, the extracellular solution contained 150 mM NaCl, 2.8 mM KCl, 1 mM $MgSO_4$, and 10 mM HEPES (pH 7.4) or 10 mM MES (pH 5.5). The pipette solution contained 130 mM $CsMeSO_3$, 15 mM CsCl, 4 mM NaCl, 5 mM BAPTA, and 10 mM HEPES (pH 7.4). For excised patch recordings, a symmetrical solution was used: 150 mM Na-gluconate, 15 mM NaCl, 5 mM EGTA, and 10 mM HEPES (pH 7.4). Solutions were applied from the microperfusion system SmartSquirt (Automate Scientific).

Stage V–VI *Xenopus laevis* oocytes were prepared as previously described (Myers et al., 2008). Oocytes were injected with 3–50 ng complementary RNA (cRNA) per oocyte and recorded 3–7 days later in normal frog Ringer's solution buffered with HEPES (pH 7.4) or MES (pH 5.5). RNA for oocyte injection was synthesized using the T7 mMessage mMachine kit (Ambion).

Binding Assay

FLAG-tagged rat TRPV1-, TRPV2-, and TRPV1(A657P)-expressing cells were induced with doxycycline for 20 hr. Membranes fractions were solubilized in TBS (200 mM NaCl, 20 mM Tris [pH 7.4]) containing 10 mM *n*-dodecyl-β-d-maltoside (DDM, Anatrace). Detergent-soluble extract was incubated with M2-FLAG resin (Sigma), washed extensively, and eluted with FLAG peptide.

For production of toxin-coupled resin, His-tagged DkTx was diluted into PBS (200 mM NaCl, 50 mM sodium phosphate [pH 7.6]) and incubated with Ni-NTA agarose resin (QIAGEN). Channel proteins were diluted into PBS containing 0.5 mM DDM and 40 mM imidazole and incubated with toxin-coupled resin for 2 hr at 4°C. Resin was then washed 3 × 10 min before elution with Laemmli SDS gel-loading buffer. Samples were separated by SDS-PAGE and were then either silver stained (SilverXpress Kit, Invitrogen) or transferred onto Immobilon-P membranes (Millipore) for western analysis.

ACCESSION NUMBERS

The GenBank accession numbers for the mature DkTx toxin sequence and the *X. laevis* TRPV1 coding region reported in this paper are HM015001 and HM015002, respectively.

REFERENCES

Alabi, A.A., Bahamonde, M.I., Jung, H.J., Kim, J.I., and Swartz, K.J. (2007). Portability of paddle motif function and pharmacology in voltage sensors. Nature 450, 370–375.

Brauchi, S., Orio, P., and Latorre, R. (2004). Clues to understanding cold sensation: thermodynamics and electrophysiological analysis of the cold receptor TRPM8. Proc. Natl. Acad. Sci. USA 101, 15494–15499.

Bulaj, G., and Olivera, B.M. (2008). Folding of conotoxins: formation of the native disulfide bridges during chemical synthesis and biosynthesis of Conus peptides. Antioxid. Redox Signal. 10, 141–155.

Catterall, W.A., Cestèle, S., Yarov-Yarovoy, V., Yu, F.H., Konoki, K., and Scheuer, T. (2007). Voltage-gated ion channels and gating modifier toxins. Toxicon 49, 124–141.

Cestèle, S., Qu, Y., Rogers, J.C., Rochat, H., Scheuer, T., and Catterall, W.A. (1998). Voltage sensor-trapping: enhanced activation of sodium channels by beta-scorpion toxin bound to the S3-S4 loop in domain II. Neuron 21, 919–931.

Chou, M.Z., Mtui, T., Gao, Y.D., Kohler, M., and Middleton, R.E. (2004). Resiniferatoxin binds to the capsaicin receptor (TRPV1) near the extracellular side of the S4 transmembrane domain. Biochemistry 43, 2501–2511.

Chuang, H.H., Neuhausser, W.M., and Julius, D. (2004). The super-cooling agent icilin reveals a mechanism of coincidence detection by a temperature-sensitive TRP channel. Neuron 43, 859–869.

Craik, D.J., Daly, N.L., and Waine, C. (2001). The cystine knot motif in toxins and implications for drug design. Toxicon 39, 43–60.

Diao, J., Lin, Y., Tang, J., and Liang, S. (2003). cDNA sequence analysis of seven peptide toxins from the spider Selenocosmia huwena. Toxicon 42, 715–723.

Doyle, D.A., Morais Cabral, J., Pfuetzner, R.A., Kuo, A., Gulbis, J.M., Cohen, S.L., Chait, B.T., and MacKinnon, R. (1998). The structure of the potassium channel: molecular basis of K+ conduction and selectivity. Science 280, 69–77.

Duda, T.F., Jr., and Palumbi, S.R. (1999). Molecular genetics of ecological diversification: duplication and rapid evolution of toxin genes of the venomous gastropod Conus. Proc. Natl. Acad. Sci. USA 96, 6820–6823.

Escoubas, P., and Rash, L. (2004). Tarantulas: eight-legged pharmacists and combinatorial chemists. Toxicon 43, 555–574.

Gavva, N.R., Klionsky, L., Qu, Y., Shi, L., Tamir, R., Edenson, S., Zhang, T.J., Viswanadhan, V.N., Toth, A., Pearce, L.V., et al. (2004). Molecular determinants of vanilloid sensitivity in TRPV1. J. Biol. Chem. 279, 20283–20295.

Gelly, J.C., Gracy, J., Kaas, Q., Le-Nguyen, D., Heitz, A., and Chiche, L. (2004). The KNOTTIN website and database: a new information system dedicated to the knottin scaffold. Nucleic Acids Res. 32(Database issue), D156–D159.

Goldstein, S.A., Pheasant, D.J., and Miller, C. (1994). The charybdotoxin receptor of a Shaker K+ channel: peptide and channel residues mediating molecular recognition. Neuron 12, 1377–1388.

Grandl, J., Hu, H., Bandell, M., Bursulaya, B., Schmidt, M., Petrus, M., and Patapoutian, A. (2008). Pore region of TRPV3 ion channel is specifically required for heat activation. Nat. Neurosci. 11, 1007–1013.

Gross, A., Abramson, T., and MacKinnon, R. (1994). Transfer of the scorpion toxin receptor to an insensitive potassium channel. Neuron 13, 961–966.

Hille, B. (2001). Ion Channels of Excitable Membranes, Third Edition (Sunderland, MA: Sinauer Associates, Inc.).

Jordt, S.E., and Julius, D. (2002). Molecular basis for species-specific sensitivity to "hot" chili peppers. Cell 108, 421–430.

Julius, D., and Basbaum, A.I. (2001). Molecular mechanisms of nociception. Nature 413, 203–210.

Kramer, R.H., and Karpen, J.W. (1998). Spanning binding sites on allosteric proteins with polymer-linked ligand dimers. Nature 395, 710–713.

Lee, H.C., Wang, J.M., and Swartz, K.J. (2003). Interaction between extracellular Hanatoxin and the resting conformation of the voltage-sensor paddle in Kv channels. Neuron 40, 527–536.

Li-Smerin, Y., and Swartz, K.J. (1998). Gating modifier toxins reveal a conserved structural motif in voltage-gated Ca2+ and K+ channels. Proc. Natl. Acad. Sci. USA 95, 8585–8589.

Li-Smerin, Y., and Swartz, K.J. (2000). Localization and molecular determinants of the Hanatoxin receptors on the voltage-sensing domains of a K(+) channel. J. Gen. Physiol. 115, 673–684.

Liang, S. (2004). An overview of peptide toxins from the venom of the Chinese bird spider Selenocosmia huwena Wang [=Ornithoctonus huwena (Wang)]. Toxicon 43, 575–585.

Long, S.B., Campbell, E.B., and Mackinnon, R. (2005). Voltage sensor of Kv1.2: structural basis of electromechanical coupling. Science 309, 903–908.

MacKinnon, R., Heginbotham, L., and Abramson, T. (1990). Mapping the receptor site for charybdotoxin, a pore-blocking potassium channel inhibitor. Neuron 5, 767–771.

Matta, J.A., and Ahern, G.P. (2007). Voltage is a partial activator of rat thermosensitive TRP channels. J. Physiol. 585, 469–482.

Milescu, M., Bosmans, F., Lee, S., Alabi, A.A., Kim, J.I., and Swartz, K.J. (2009). Interactions between lipids and voltage sensor paddles detected with tarantula toxins. Nat. Struct. Mol. Biol. 16, 1080–1085.

Miller, C. (1995). The charybdotoxin family of K+ channel-blocking peptides. Neuron 15, 5–10.

Myers, B.R., Bohlen, C.J., and Julius, D. (2008). A yeast genetic screen reveals a critical role for the pore helix domain in TRP channel gating. Neuron 58, 362–373.

Phillips, E., Reeve, A., Bevan, S., and McIntyre, P. (2004). Identification of species-specific determinants of the action of the antagonist capsazepine and the agonist PPAHV on TRPV1. J. Biol. Chem. 279, 17165–17172.

Phillips, L.R., Milescu, M., Li-Smerin, Y., Mindell, J.A., Kim, J.I., and Swartz, K.J. (2005). Voltage-sensor activation with a tarantula toxin as cargo. Nature 436, 857–860.

Ramsey, I.S., Delling, M., and Clapham, D.E. (2006). An introduction to TRP channels. Annu. Rev. Physiol. 68, 619–647.

Roy, A., Zhou, X., Chong, M.Z., D'hoedt, D., Foo, C.S., Rajagopalan, N., Nirthanan, S., Bertrand, D., Sivaraman, J., and Kini, R.M. (2010). Structural and functional characterization of a novel homodimeric three-finger neurotoxin from the venom of Ophiophagus hannah (king cobra). J. Biol. Chem. 285, 8302–8315.

Schmidt, D., and MacKinnon, R. (2008). Voltage-dependent K+ channel gating and voltage sensor toxin sensitivity depend on the mechanical state of the lipid membrane. Proc. Natl. Acad. Sci. USA *105*, 19276–19281.

Siemens, J., Zhou, S., Piskorowski, R., Nikai, T., Lumpkin, E.A., Basbaum, A.I., King, D., and Julius, D. (2006). Spider toxins activate the capsaicin receptor to produce inflammatory pain. Nature *444*, 208–212.

Sokolov, S., Kraus, R.L., Scheuer, T., and Catterall, W.A. (2008). Inhibition of sodium channel gating by trapping the domain II voltage sensor with protoxin II. Mol. Pharmacol. *73*, 1020–1028.

Swartz, K.J. (2007). Tarantula toxins interacting with voltage sensors in potassium channels. Toxicon *49*, 213–230.

Swartz, K.J. (2008). Sensing voltage across lipid membranes. Nature *456*, 891–897.

Swartz, K.J., and MacKinnon, R. (1997). Mapping the receptor site for hanatoxin, a gating modifier of voltage-dependent K+ channels. Neuron *18*, 675–682.

Takahashi, H., Kim, J.I., Min, H.J., Sato, K., Swartz, K.J., and Shimada, I. (2000). Solution structure of hanatoxin1, a gating modifier of voltage-dependent K(+) channels: common surface features of gating modifier toxins. J. Mol. Biol. *297*, 771–780.

Terlau, H., and Olivera, B.M. (2004). Conus venoms: a rich source of novel ion channel-targeted peptides. Physiol. Rev. *84*, 41–68.

Tombola, F., Pathak, M.M., and Isacoff, E.Y. (2006). How does voltage open an ion channel? Annu. Rev. Cell Dev. Biol. *22*, 23–52.

Tsetlin, V., Utkin, Y., and Kasheverov, I. (2009). Polypeptide and peptide toxins, magnifying lenses for binding sites in nicotinic acetylcholine receptors. Biochem. Pharmacol. *78*, 720–731.

Ueberheide, B.M., Fenyö, D., Alewood, P.F., and Chait, B.T. (2009). Rapid sensitive analysis of cysteine rich peptide venom components. Proc. Natl. Acad. Sci. USA *106*, 6910–6915.

Venkatachalam, K., and Montell, C. (2007). TRP channels. Annu. Rev. Biochem. *76*, 387–417.

Voets, T., Droogmans, G., Wissenbach, U., Janssens, A., Flockerzi, V., and Nilius, B. (2004). The principle of temperature-dependent gating in cold- and heat-sensitive TRP channels. Nature *430*, 748–754.

Walker, C.S., Jensen, S., Ellison, M., Matta, J.A., Lee, W.Y., Imperial, J.S., Duclos, N., Brockie, P.J., Madsen, D.M., Isaac, J.T., et al. (2009). A novel Conus snail polypeptide causes excitotoxicity by blocking desensitization of AMPA receptors. Curr. Biol. *19*, 900–908.

Wang, S.Y., and Wang, G.K. (2003). Voltage-gated sodium channels as primary targets of diverse lipid-soluble neurotoxins. Cell. Signal. *15*, 151–159.

Yeh, B.I., Kim, Y.K., Jabbar, W., and Huang, C.L. (2005). Conformational changes of pore helix coupled to gating of TRPV5 by protons. EMBO J. *24*, 3224–3234.

Yu, L., Sun, C., Song, D., Shen, J., Xu, N., Gunasekera, A., Hajduk, P.J., and Olejniczak, E.T. (2005). Nuclear magnetic resonance structural studies of a potassium channel-charybdotoxin complex. Biochemistry *44*, 15834–15841.

Zhu, S., Darbon, H., Dyason, K., Verdonck, F., and Tytgat, J. (2003). Evolutionary origin of inhibitor cystine knot peptides. FASEB J. *17*, 1765–1767.